INSTITUTE OF PHYSICS PUBLISHING JOURNAL OF PHYSICS B: ATOMIC, MOLECULAR AND OPTICAL PHYSICS

J. Phys. B: At. Mol. Opt. Phys. **38** (2005) 635–643 doi:10.1088/0953-4075/38/6/002

Photo double ionization of helium 100 eV and 450 eV above threshold: II. Circularly polarized light

A Knapp[1], A Kheifets[2], I Bray[3], Th Weber[1,5,6], A L Landers[4], S Schössler[1], T Jahnke[1], J Nickles[1], S Kammer[1], O Jagutzki[1], L Ph H Schmidt[1], M Schöffler[1], T Osipov[5,6], M H Prior[6], H Schmidt-Böcking[1], C L Cocke[5] and R Dörner[1]

[1] Institut für Kernphysik, Universität Frankfurt, August-Euler-Str 6, D-60486 Frankfurt, Germany
[2] Research School of Physical Sciences and Engineering, Australian National University, Canberra ACT 0200, Australia
[3] Centre for Atomic, Molecular and Surface Physics, Murdoch University, Perth 6150, Australia
[4] Physics Department, Auburn University, Auburn, AL 36849, USA
[5] Deptartment of Physics, Kansas State University, Cardwell Hall, Manhattan KS 66506, USA
[6] Lawrence Berkeley National Lab., Berkeley, CA 94720, USA

E-mail: doerner@atom.uni-frankfurt.de

Received 30 November 2004
Published 7 March 2005
Online at stacks.iop.org/JPhysB/38/635

Abstract

We present a joint experimental and theoretical study of the fully differential cross section of the photo double ionization of helium with left and right circularly polarized light at $E_{\mathrm{exc}} = 100$ eV and 450 eV above the threshold. We analyse angular distributions for the slow electron and the normalized circular dichroism for various energy sharings of the excess energy between the two electrons. The experimental results are well reproduced by convergent close coupling calculations.

1. Introduction

The chirality is a property of an object that is not identical to its mirror image. More precisely, a chiral object cannot be mapped to its mirror image by rotations and/or translations alone. One might think that chirality in an ionization process occurs solely if one deals with a complex target or if the spin is relevant, and hence would not be found for the case of spherically symmetric ground state ($^1S^e$) helium atoms. However, Berakdar and Klar [1, 2] have pointed out that one can find chirality in the photo double ionization (PDI) of helium with circularly polarized light. The axial vector of the rotating electric field and the momenta of both electrons lead to a handedness if the following conditions are fulfilled: first, the electrons must be distinguishable ($E_1 \neq E_2$, E_1 and E_2 are energies of electron 1 and electron 2,

 © 2005 IOP Publishing Ltd Printed in the UK

respectively). Second, their momenta $\boldsymbol{p}_1$ and $\boldsymbol{p}_2$ must not be parallel or antiparallel. And third, both momentum vectors and the momentum of light $\boldsymbol{k}$ must not be in the same plane ($\boldsymbol{p}_1 \times \boldsymbol{p}_2 = \boldsymbol{n}$ and $\boldsymbol{n}$ not $\perp \boldsymbol{k}$). In short, the axial vector of the rotating electric field and the two electron momenta must generate a left-handed or right-handed tripod with distinguishable legs. The chirality is quantified by a so-called circular dichroism. Two slightly different, though connected definitions of the circular dichroism have been established in the literature: first, the circular dichroism

$$\mathrm{CD}(E_1, E_2, \Theta_1, \Theta_2, \Phi_{12}) = 4\mathrm{DCS}_{\sigma^+} - 4\mathrm{DCS}_{\sigma^-}, \tag{1}$$

and second, the normalized circular dichroism

$$\mathrm{CD_n}(E_1, E_2, \Theta_1, \Theta_2, \Phi_{12}) = \frac{4\mathrm{DCS}_{\sigma^+} - 4\mathrm{DCS}_{\sigma^-}}{4\mathrm{DCS}_{\sigma^+} + 4\mathrm{DCS}_{\sigma^-}}. \tag{2}$$

Here Θ_1, Θ_2 are the polar angles of electrons 1 and 2 with respect to the propagation direction of light and Φ_{12} is the difference of the corresponding azimuthal angles of both electrons around the light propagation which is perpendicular to the momentum vectors of both electrons. $4\mathrm{DCS}_{\sigma^+}$ and $4\mathrm{DCS}_{\sigma^-}$ are the fourfold differential cross sections (4DCS) $\mathrm{d}^4\sigma/(\mathrm{d}E_1\, \mathrm{dcos}\,\Theta_1\, \mathrm{dcos}\,\Theta_2\, \mathrm{d}\Phi_{12})$ of the PDI of helium from right and left circularly polarized light. These 4DCS are fully differential within the dipole approximation. For comparing the magnitude of the circular dichroism in the case of different energy sharing or different photon energies, the use of $\mathrm{CD_n}$ is better suited.

To study the circular dichroism CD or the normalized circular dichroism $\mathrm{CD_n}$, the 4DCS of the PDI of helium with circularly polarized light is needed. In principle, only the 4DCS of either left or right circularly polarized light is required because of the symmetry consideration [3]:

$$4\mathrm{DCS}_{\sigma^+}(E_1, E_2, \Theta_1, \Theta_2, \Phi_{12}) = 4\mathrm{DCS}_{\sigma^-}(E_1, E_2, \Theta_1, \Theta_2, 360^\circ - \Phi_{12}). \tag{3}$$

On the other hand, measuring $4\mathrm{DCS}_{\sigma^+}$ as well as $4\mathrm{DCS}_{\sigma^-}$ allows a rudimentary consistency check using equation (3). In addition, equation (3) in combination with equation (2) shows that the circular dichroism is point symmetric with respect to $\Phi_{12} = 180^\circ$.

The first coincident PDI experiment concerning CD was performed by Viefhaus *et al* [4] at $E_{\mathrm{exc}} = 14.5$ eV above the threshold. They measured $\mathrm{CD_n}$ at three different angles $\Phi_{12} = 85^\circ$, 125° and 150° and five energy sharings. In the following years, more measurements were performed at the excess energies $E_{\mathrm{exc}} = 9$, 20 and 60 eV (Achler *et al* [5], Collins *et al* [6], Mergel *et al* [7] and Soejima *et al* [8]).

In the present paper, we report our measurements of the 4DCS with left and right circularly polarized light (Stokes parameter $S_3 = \pm 0.99$) at the excess energies $E_{\mathrm{exc}} = 100$ eV and $E_{\mathrm{exc}} = 450$ eV above the PDI threshold. The experiments were performed at Beamline 4.0.2 of the Advanced Light Source at the Lawrence Berkeley National Laboratory [9]. The 4DCS were obtained by measuring the three-dimensional momentum vectors of one electron and the He^{2+} ion in coincidence using the COLTRIMS method [10]. The purpose of the present study is to compare the 4DCS with circularly and linearly polarized light (see companion paper I immediately preceding this one) as well as with an *ab initio* convergent close-coupling calculation (CCC). Furthermore, the angular and energy dependence of $\mathrm{CD_n}$ will be shown. Finally, a consistency check, first suggested by Berakdar [11], will be presented that shows the reliability of our two data sets gained with linearly and circularly polarized light. A complete

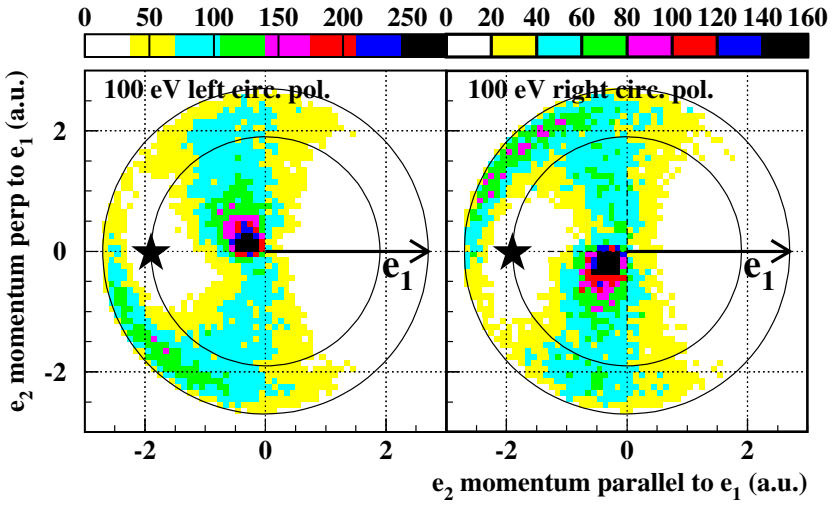

Figure 1. Momentum distribution of the second electron e_2 with respect to the first electron e_1 for $E_{exc} = 100$ eV above the threshold. The two electrons are in a plane perpendicular to the light propagation x: $\Theta_1 = \Theta_2 = 90^\circ \pm 30^\circ$. The arrow indicates the direction of the first electron e_1. The outer circle is the maximum possible momentum. The inner circle indicates the locus of events with equal energy sharing. The star marks the node at $\boldsymbol{p}_1 = -\boldsymbol{p}_2$ (selection rule C). This figure can be compared to figure 5 in paper 1 which shows the analogous data for linearly polarized light.

(This figure is in colour only in the electronic version)

description of our experimental set-up, the normalization of the PDI data and the CCC theory can be found in our companion paper I preceding this one.

2. Results

2.1. Overview

An overview of the three particle dynamics in the final state for $E_{exc} = 100$ eV is given in figure 1. The density plot shows the momentum distribution for the complementary electron e_2 for a fixed direction of the electron e_1 indicated by the arrow. Both electrons are chosen to be perpendicular to the light propagation, which is perpendicular to the plane of the diagram. In the left (right) panel, the light is left (right) circularly polarized. The outer circle indicates the locus where electron e_2 carries all the excess energy of 100 eV and the inner circle shows the locus where each electron has 50 eV energy.

In figure 1, the structure of the observed momentum distribution is dominated by two physical effects. Due to the electron repulsion, the electrons are mainly emitted into opposite half spheres. Furthermore, the final state symmetry ($^1P^o$) leads to a node (marked by a star in both panels) at $\boldsymbol{p}_1 = -\boldsymbol{p}_2$ (selection rule C, predicted by Maulbetsch and Briggs [12]). This figure should be compared with figure 5 of paper I where the analogous data with linearly polarized light are presented. In contrast to the result from linearly polarized light at the same excess energy, the momentum distribution with circularly polarized light is not symmetric to the horizontal axis which is parallel to the fixed electron momentum. Furthermore, the momentum distribution shows a vortex structure. This structure has nothing to do with any selection rules but is a direct consequence of the dynamics of the photoelectrons liberated by circularly polarized light.

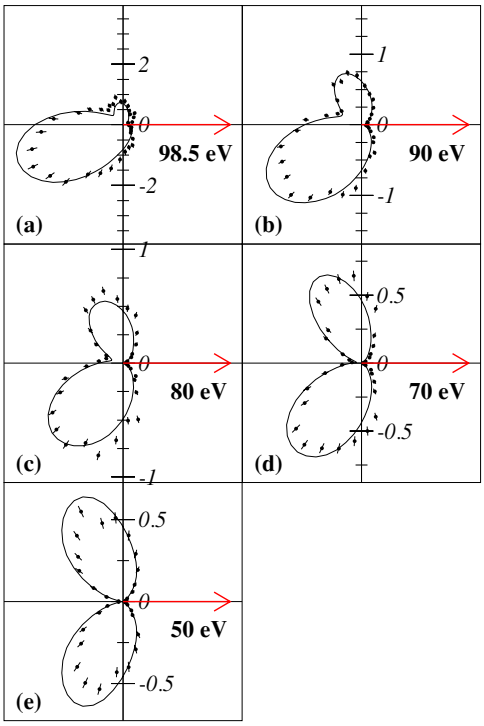

Figure 2. Fourfold differential cross section of the He PDI at $E_\gamma = 179$ eV photon energy on the absolute scale in barn/(eV rad). The two electrons are in a plane perpendicular to the light propagation x: $\Theta_1 = \Theta_2 = 90^\circ \pm 7^\circ$. The direction and the energy of one of the two electrons are fixed as indicated by the number and the arrow. The polar plots show the angular distribution of the complementary electron. The solid line is a CCC calculation in the velocity form. The measurements are normalized to the precisely measured cross section by Samson *et al*. The 4DCS of the left circularly polarized light is mirrored and added to the 4DCS of the right circularly polarized light. Energy integration: (a) $97 < E_1 < 100$ eV, (b) $85 < E_1 < 95$ eV, (c) $75 < E_1 < 85$ eV, (d) $65 < E_1 < 75$ eV, (e) $45 < E_1 < 55$ eV.

2.2. 100 eV excess energy

For a closer inspection and a more thorough comparison with theory, the 4DCS with right circularly polarized light are presented in figure 2 for different energy sharings. The absolute scale and the common polar and azimuthal angles are used on all panels. In order to gain statistics, we have added the events from the two experiments with left and right circularly polarized light in accordance with equation (3). The two electrons are in a plane perpendicular to the light propagation x: $\Theta_1 = \Theta_2 = 90^\circ \pm 7^\circ$. Figure 2 shows the angular distribution of the complementary electron with respect to the fixed angle reference electron direction indicated by an arrow. The solid line in each panel is the velocity form of the CCC calculation. Figure 2 shows the 4DCS dependence on the energy sharing. For $E_{\rm exc} = 100$ eV data we chose the following five energy sharings: 1.5 eV $\leftrightarrow$ 98.5 eV; 10 eV $\leftrightarrow$ 90 eV; 20 eV $\leftrightarrow$ 80 eV; 30 eV $\leftrightarrow$ 70 eV and 50 eV $\leftrightarrow$ 50 eV.

In figures 2(a)–(d), the circular dichroism can be seen qualitatively. At equal energy sharing, the angular distribution is symmetric relative to the horizontal axis. Because the two electrons are indistinguishable, the circular dichroism vanishes (figure 2(e)). The angular distribution consists of two equal size lobes and the node arising from selection rule C can be

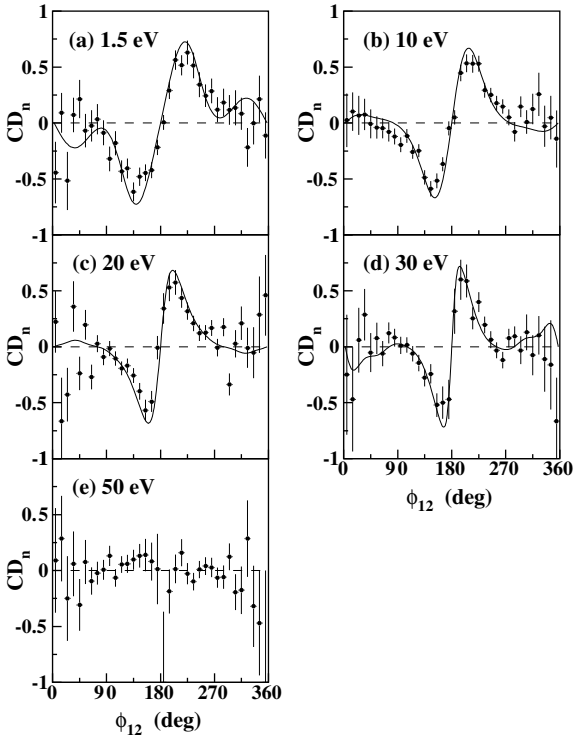

Figure 3. CD_n as a function of Φ_{12} for five different energy sharings 100 eV above the threshold. The two electrons are in a plane perpendicular to the light propagation x: $\Theta_1 = \Theta_2 = 90^\circ \pm 7^\circ$. Energy integration: (a) $97 < E_1 < 100$ eV, (b) $85 < E_1 < 95$ eV, (c) $75 < E_1 < 85$ eV, (d) $65 < E_1 < 75$ eV, (e) $45 < E_1 < 55$ eV. The solid line is a CCC calculation in the velocity form.

seen. At a slightly more asymmetric energy sharing, the lobe in the second quadrant scales down while the lobe in the third quadrant grows (figures 2(c) and (d)). At a more asymmetric energy sharing $E_1 = 98.5$ eV (figure 2(a)), the lobe in the second quadrant is barely visible, so that we can almost say that the angular distribution of the slow electron consists of only one lobe. The CCC calculation yields good agreement with our experimental results.

To study CD in a quantitative way, we examine CD_n (figure 3). At equal energy sharing we find a vanishing CD_n. For the other panels (figures 3(a)–(d)) there is quite a strong CD_n; its maximum value $CD_{n,max} \simeq 0.7$ is almost the same for all panels (a–d). The Φ_{12} position of $CD_{n,max}$, however, depends on the energy sharing. Because CD_n is point symmetric around $\Phi_{12} = 180^\circ$ we consider just the range between $\Phi_{12} = 0^\circ$ and $\Phi_{12} = 180^\circ$. At extreme unequal energy sharing (figure 3(a)), we find $CD_{n,max}$ at an angle of $\Phi_{12} \cong 140^\circ$. At more equal energy sharing the locus of $CD_{n,max}$ is shifted to larger angles Φ_{12}. At an energy sharing of 30 eV $\leftrightarrow$ 70 eV (figure 3(d)), we find $CD_{n,max}$ at an angle of $\Phi_{12} \cong 170^\circ$. The shift of $CD_{n,max}$ for more symmetric energy sharing to $\Phi_{12} \approx 180^\circ$ causes a steeper slope at $\Phi_{12} = 180^\circ$.

Comparing our result with the CD experiments 20 eV above threshold (Achler *et al* [5]) we find the following: for 20 eV and 100 eV there is a constant $CD_{n,max}$ for almost all unequal energy sharings both in theory and experiment. For 20 eV above threshold there is a $CD_{n,max} \cong 0.7$ (experiment), CCC calculates a $CD_{n,max} \cong 0.9$, which is a bit higher than the experimental results. According to Berakdar [3], CD_n decreases as $E_{exc}^{1/2}$ right at the threshold

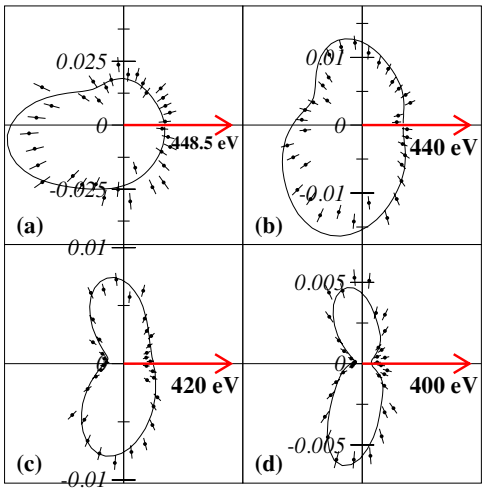

Figure 4. Fourfold differential cross section of the He PDI at 529 eV photon energy normalized to the CCC calculation in barn/(eV rad). The two electrons are in a plane perpendicular to the light propagation x: $\Theta_1 = \Theta_2 = 90^\circ \pm 20^\circ$. The direction and the energy of one of the two electrons are fixed as indicated by the number and the arrow. The polar plots show the angular distribution of the complementary electron. The solid line is a CCC calculation in the velocity form. The 4DCS of the left circularly polarized light is mirrored and added to the 4DCS of the right circularly polarized light. Energy integration: (a) $447 < E_1 < 450$ eV, (b) $434 < E_1 < 446$ eV, (c) $410 < E_1 < 430$ eV, (d) $390 < E_1 < 410$ eV.

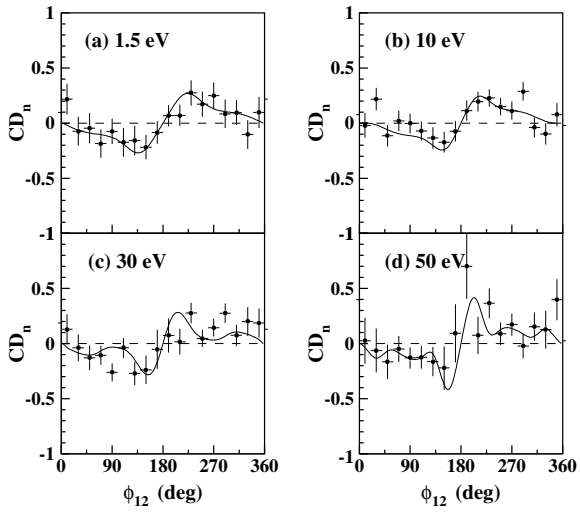

Figure 5. CD_n 450 eV above the threshold. The two electrons are in a plane perpendicular to the light propagation x: $\Theta_1 = \Theta_2 = 90^\circ \pm 20^\circ$. Energy integration: (a) $447 < E_1 < 450$ eV, (b) $434 < E_1 < 446$ eV, (c) $410 < E_1 < 430$ eV, (d) $390 < E_1 < 410$ eV. The solid line is a CCC calculation in the velocity form.

$E_{\rm exc} \to 0$ and is proportional to $E_{\rm exc}^{-1/2}$ for high photon energies $E_{\rm exc} \to \infty$. It remains open at which photon energy a decrease of CD_n is to be expected.

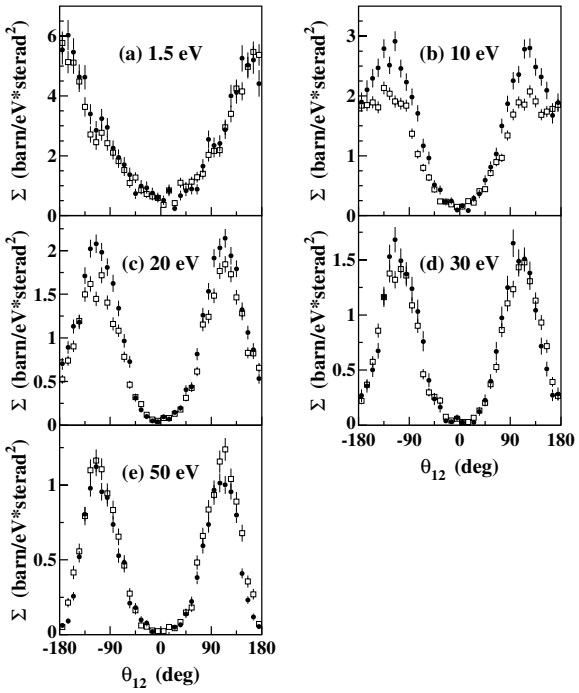

Figure 6. Consistency check. the full circles: linearly polarized light $4\mathrm{DCS}_{\varepsilon_x}$ + $4\mathrm{DCS}_{\varepsilon_y}$; open squares: circularly polarized light $4\mathrm{DCS}_{\sigma^+}$ + $4\mathrm{DCS}_{\sigma^-}$. Circularly polarized light: the two electrons are in a plane perpendicular to the light propagation x: $\Theta_1 = \Theta_2 = 90^\circ \pm 7^\circ$. Energy integration: (a) $97 < E_1 < 100$ eV, (b) $85 < E_1 < 95$ eV, (c) $75 < E_1 < 85$ eV, (d) $65 < E_1 < 75$ eV, (e) $45 < E_1 < 55$ eV. Linearly polarized light ε_x; the complementary electron is within $\pm 5^\circ$ (a, b, d) and $\pm 10^\circ$ (c,e) in the plane: (a) $97 < E_1 < 100$ eV, $-5^\circ < \Theta_1 < 5^\circ$, (b) $85 < E_1 < 95$ eV, $-5^\circ < \Theta_1 < 5^\circ$, (c) $75 < E_1 < 85$ eV, $-5^\circ < \Theta_1 < 5^\circ$, (d) $65 < E_1 < 75$ eV, $-5^\circ < \Theta_1 < 5^\circ$, (e) $45 < E_1 < 55$ eV, $-5^\circ < \Theta_1 < 5^\circ$. Linearly polarized light ε_y: the angle between the polarization axis and the fixed electron is $\Theta_1 = (90 \pm 5)^\circ$, the complementary electron is within the plane defined by the polarization vector and the fixed electron within $\pm 15^\circ$. (a) $97 < E_1 < 100$ eV, (b) $85 < E_1 < 95$ eV, (c) $75 < E_1 < 85$ eV, (d) $65 < E_1 < 75$ eV, (e) $45 < E_1 < 55$ eV.

2.3. 450 eV excess energy

We now present the angular distributions for various energy sharings at $E_{\mathrm{exc}} = 450$ eV (figure 4). The two electrons are in a plane perpendicular to the light propagation x: $\Theta_1 = \Theta_2 = 90^\circ \pm 20^\circ$. We selected the following energy sharings: 1.5 eV $\leftrightarrow$ 448.5 eV; 10 eV $\leftrightarrow$ 440 eV; 30 eV $\leftrightarrow$ 420 eV and 50 eV $\leftrightarrow$ 400 eV.

At a glance, the angular distributions are not symmetric to the horizontal axis. Therefore we should expect a noticeable, albeit small, CD. The angular distribution of the slow electron at the extreme unequal energy sharing consists only of one lobe. The angular distribution is almost isotropic and nearly symmetric to the horizontal axis (figure 4(a)). At an energy sharing of 50 eV $\leftrightarrow$ 400 eV the formation of two lobes is visible (figure 4(d)). The formation of the two lobes should be compared to figure 9 of paper I. The two lobes are not a result of selection rule C, but a result of the TS1 mechanism [13, 14] which dominates at these energy sharings [15].

Figure 5 shows the normalized circular dichroism $\mathrm{CD_{n.}}$. One sees that the $\mathrm{CD_{n,max}}$ at 450 eV above the threshold, for all energy sharings, is much smaller than for the 100 eV case.

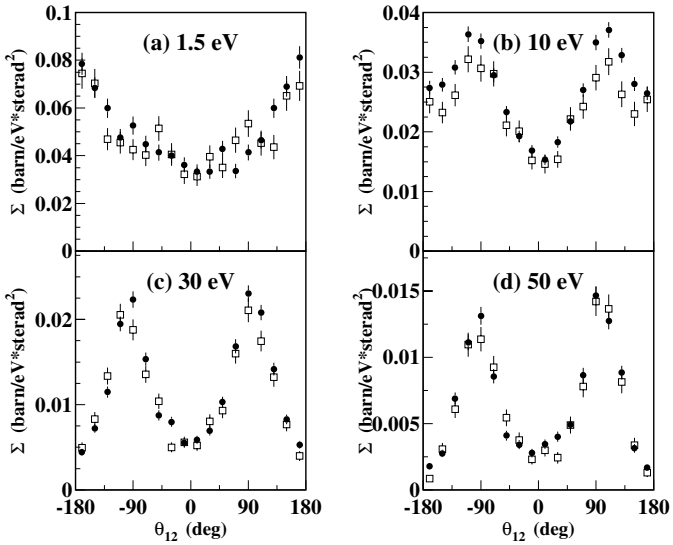

Figure 7. Consistency check. The full circles: linearly polarized light $4\mathrm{DCS}_{\varepsilon_x} + 4\mathrm{DCS}_{\varepsilon_y}$; open squares: circularly polarized light $4\mathrm{DCS}_{\sigma^+} + 4\mathrm{DCS}_{\sigma^-}$. Circularly polarized light: the two electrons are in a plane perpendicular to the light propagation x: $\Theta_1 = \Theta_2 = 90^\circ \pm 20^\circ$. Energy integration: (a) $447 < E_1 < 450$ eV, (b) $434 < E_1 < 446$ eV, (c) $410 < E_1 < 430$ eV, (d) $390 < E_1 < 410$ eV. Linearly polarized light ε_x; the complementary electron is within $\pm 20^\circ$ in the plane: (a) $447 < E_1 < 500$ eV, $-25^\circ < \Theta_1 < 25^\circ$, (b) $434 < E_1 < 446$ eV, $-30^\circ < \Theta_1 < 30^\circ$, (c) $410 < E_1 < 430$ eV, $-25^\circ < \Theta_1 < 25^\circ$, (d) $390 < E_1 < 410$ eV, $-30^\circ < \Theta_1 < 30^\circ$. Linearly polarized light ε_y: the angle between the polarization axis and the fixed electron is $\Theta_1 = (90 \pm 20)^\circ$, the complementary electron is within the plane defined by the polarization vector and the fixed electron within $\pm 25^\circ$. (a) $447 < E_1 < 450$ eV, (b) $434 < E_1 < 446$ eV, (c) $410 < E_1 < 430$ eV, (d) $390 < E_1 < 410$ eV.

Figures 5(a) and (b) show a maximum value of $\mathrm{CD}_{\mathrm{n,max}} \simeq 0.2$. The experimental results are in good agreement with CCC calculations. In figures 5(c) and (d), however, the statics are too poor to give any reliable information about CD_{n}. The CCC calculation predicts a higher $\mathrm{CD}_{\mathrm{n,max}}$ for more symmetric energy sharing. For an energy sharing of 30 eV $\leftrightarrow$ 420 eV and 50 eV $\leftrightarrow$ 400 eV, we cannot draw any conclusion about the higher $\mathrm{CD}_{\mathrm{n,max}}$ compared to more extreme asymmetric energy sharings.

2.4. Consistency checks

As already mentioned, a first consistency check can be made by applying equation (3). In the absence of systematic errors, the shape of CD_{n} must be point symmetric to $\Phi_{12} = 180^\circ$. Our data in figures 3(a)–(e) and figures 5(a) and (b) fulfil this requirement within the statistical error bars. Berakdar [11] suggested a second consistency check relating data for circularly and linearly polarized light. He showed that the sum of $4\mathrm{DCS}_{\sigma^-}$ and $4\mathrm{DCS}_{\sigma^+}$ is identical to the sum of the 4DCS for linear polarized light with the polarization axis being parallel ($4\mathrm{DCS}_{\varepsilon_x}$) and perpendicular ($4\mathrm{DCS}_{\varepsilon_y}$) to the horizontal axis, respectively:

$$\Sigma = 4\mathrm{DCS}_{\varepsilon_x} + 4\mathrm{DCS}_{\varepsilon_y} = 4\mathrm{DCS}_{\sigma^-} + 4\mathrm{DCS}_{\sigma^+}. \tag{4}$$

Figures 6 and 7 show this consistency check for the data from this paper and those from paper I for 100 eV and 450 eV, respectively. In figure 6, the full circles and the open squares are $4\mathrm{DCS}_{\varepsilon_x} + 4\mathrm{DCS}_{\varepsilon_y}$ and $4\mathrm{DCS}_{\sigma^-} + 4\mathrm{DCS}_{\sigma^+}$, respectively. The energy and solid angle

acceptance for the circular data are the same as in figure 3 as well as in figures 6 and figure 8 of our companion paper (paper I). In figure 7, the full circles and the open squares are again $4DCS_{\varepsilon_x} + 4DCS_{\varepsilon_y}$ and $4DCS_{\sigma^-} + 4DCS_{\sigma^+}$, respectively. The energy and solid angle integration for the circular data are the same as in figure 5; the integration for the linearly polarized light are the same as in figures 9 and 11 of our companion paper (paper I). For both photon energies $4DCS_{\varepsilon_x} + 4DCS_{\varepsilon_y}$ and $4DCS_{\sigma^-} + 4DCS_{\sigma^+}$ are in good agreement.

In summary, we have presented the angular distributions and the CD_n for 100 eV and 450 eV above threshold. The 450 eV CD_n is much smaller than the 100 eV CD_n, though still observable. A general consistency check has been applied on the two data sets for linearly and circularly polarized light. The CCC calculations give a good description of the experimental data.

Acknowledgments

This work was supported in part by BMBF, DFG, the Division of Chemical Sciences, Geosciences and Biosciences Division, Office of Basic Energy Sciences, Office of Science, US Department of Energy. A Knapp thanks Graduiertenförderung des Landes Hessen for financial support. Th Weber thanks Graduiertenfoerderung des Landes Hessen as well as the Alexander von Humboldt Foundation for financial support. We thank E Arenholz and T Young and the staff of the Advanced Light Source for extraordinary support during our beam time. The CCC computations presented in this paper were performed using the Compaq AlphaServer SC National Facility of the Australian Partnership for Advanced Computing.

References

[1] Berakdar J and Klar H 1992 *Phys. Rev. Lett.* **69** 1175
[2] Berakdar J, Klar H, Huetz A and Selles P 1993 *J. Phys. B: At. Mol. Opt. Phys.* **26** 1463
[3] Berakdar J 1998 *J. Phys. B: At. Mol. Opt. Phys.* **31** 3167
[4] Viefhaus J *et al* 1996 *Phys. Rev. Lett.* **77** 3975
[5] Achler M, Mergel V, Spielberger L, Azuma Y, Dörner R and Schmidt-Böcking H 2001 *J. Phys. B: At. Mol. Opt. Phys.* **34** 965
[6] Collins S A *et al* 2002 *Phys. Rev.* A **65** 052717
[7] Mergel V *et al* 1998 *Phys. Rev. Lett.* **80** 5301
[8] Soejima K, Danjo A, Okuno K and Yagishita A 1999 *Phys. Rev. Lett.* **83** 1546
[9] Young A T *et al* 2001 *Nucl. Instrum. Methods. A* **549** 467
[10] Dörner R, Mergel V, Jagutzki O, Spielberger L, Ullrich J, Moshammer R and Schmidt-Böcking H 2000 *Phys. Rep.* **330** 96–192
[11] Berakdar J 1999 *J. Phys. B: At. Mol. Opt. Phys.* **32** L27
[12] Maulbetsch F and Briggs J S 1995 *J. Phys. B: At. Mol. Opt. Phys.* **28** 551
[13] Carlson T A 1967 *Phys. Rev.* **156** 142
[14] Samson J A R 1990 *Phys. Rev. Lett.* **65** 2861
[15] Knapp A *et al* 2002 *Phys. Rev. Lett.* **89** 033004